RadioGraphics

Developmental Lung Anomalies in the Adult: Radiologic-Pathologic Correlation[1]

Carl J. Zylak, MD, FRCPC • William R. Eyler, MD • David L. Spizarny, MD • Chad H. Stone, MD

CME FEATURE

See accompanying test at http://www.rsna.org/education/rg_cme.html

LEARNING OBJECTIVES FOR TEST 2

After reading this article and taking the test, the reader will be able to:

- Discuss the embryogenesis of the lung.
- Recognize the imaging characteristics of the common developmental anomalies in the adult.
- Differentiate anomalies from more sinister abnormalities.

SUPPLEMENTAL MATERIAL

Additional figures to supplement this article are available online at radiographics.rsnajnls.org/cgi/content/full/22/S25/DC1.

Encountering a developmental lung anomaly in the adult can be a challenge, as the abnormality may be mistaken for something more sinister. The common anomalies encountered are classified into three broad categories: bronchopulmonary (lung bud) anomalies, vascular anomalies, and combined lung and vascular anomalies. The imaging features of these developmental anomalies at conventional radiography, ventilation-perfusion lung nuclear scanning, angiography, computed tomography, and magnetic resonance imaging are useful in differential diagnosis of thoracic lesions. Lung bud anomalies include agenesis, congenital bronchial atresia, congenital lobar emphysema, congenital cystic adenomatoid malformation, pulmonary bronchogenic cysts, tracheal or pig bronchus, and accessory cardiac bronchus. Vascular anomalies include interruption or absence of a main pulmonary artery, anomalous origin of the left pulmonary artery from the right, anomalous pulmonary venous drainage (partial or complete), and pulmonary arteriovenous malformation. Combined lung and vascular anomalies include the hypogenetic lung (scimitar) syndrome and bronchopulmonary sequestration, both intralobar and extralobar.

Index terms: Bronchi, abnormalities, 60.14 • Lung, abnormalities, 60.14 • Lung, congenital malformation, 60.14 • Pulmonary arteries, abnormalities, 564.15, 944.141 • Pulmonary veins, abnormalities, 565.15, 945.142

RadioGraphics 2002; 22:S25–S43

[1]From the Departments of Diagnostic Radiology (C.J.Z., W.R.E., D.L.S.) and Anatomic Pathology (C.H.S.), Henry Ford Hospital, 2799 W Grand Blvd, Detroit, MI 48202-2689. Presented as an education exhibit at the 2000 RSNA scientific assembly. Received January 21, 2002; revision requested February 20 and received April 15; accepted April 26. **Address correspondence to** C.J.Z. (e-mail: *zylak@rad.hfh.edu*).

Introduction

Developmental anomalies of the lung are usually detected in the neonatal period and in early childhood. However, some are not encountered until later childhood or adulthood. As some of these anomalies can be confused with more sinister abnormalities, an understanding of their imaging features will facilitate this distinction.

Anomalies encountered in adulthood can be classified into three broad categories: bronchopulmonary (lung bud) anomalies, vascular anomalies, and combined lung and vascular anomalies. This article highlights the common anomalies encountered in each of these categories.

Embryology

Lung

The development and growth of the lung consist of two stages, the intrauterine and the postnatal. Intrauterine development has been divided into four periods: embryonic, pseudoglandular, canalicular, and saccular (alveolar).

During the embryonic period, the development of the lung begins at approximately 26 days gestation as a ventral diverticulum of the foregut near the junction of the occipital and cervical segments (see Fig S1 at *radiographics.rsnajnls.org/cgi/content/full/22/S25/DC1*). This outpouching is lined by endodermal epithelium and is invested by splanchnic mesenchyme. For the next 2 days, the right and left lung buds arise from this outpouching with a characteristic direction of growth, that on the right being directed caudally and that on the left more transversely. The respiratory portion of the gut becomes separated from the esophageal portion by lateral ingrowths of the surrounding mesoderm that meet to form the tracheoesophageal septum. Within a few additional days, the lung buds have elongated into primary lung sacs and the five lobar bronchi appear as outgrowths of the primary bronchi. These events occur approximately by the end of the 5th week, marking the end of the embryonic period.

The pseudoglandular period extends from the 5th week of gestation to the 16th week and is primarily related to development of the bronchial tree. The five lobar bronchi branch in a more or less dichotomous fashion, with approximately 70% of the bronchial branching having occurred between the 10th and 14th weeks. By the 16th week, virtually all of the conducting airways are present. During this period, the airways are blind tubules lined by columnar or cuboidal epithelium, hence the term *pseudoglandular*.

Cartilage may be seen within the trachea as early as 7 weeks gestation. It develops in the bronchi in a centrifugal direction. The canalicular period is from the 17th week to the 25th–28th week and represents the early stages of development of transitional airways. Mesenchymal tissue decreases; air spaces and newly formed capillaries approximate one another.

In the saccular (alveolar) period, acinar morphology is well developed by the 28th week of gestation. Alveoli have been demonstrated as early as 30 weeks gestation. The final period of normal intrauterine lung development from 36 weeks to term includes the prolific development of alveoli.

In the postnatal period, alveolar development occurs to 8 years of age. The air-tissue interface is 3–4 m^2 at birth, 32 m^2 by 8 years of age, and 75 m^2 by adulthood. Conducting airways increase in proportion to body size.

Pulmonary Arteries

The pulmonary artery develops from the sixth aortic arch (see Fig S2 at *radiographics.rsnajnls.org/cgi/content/full/22/S25/DC1*). The proximal part of the arch becomes the proximal segment of the right and left pulmonary arteries. On the right side, the distal part loses its connection with the arch, whereas on the left it maintains its connection as the ductus arteriosus.

During the embryonic and pseudoglandular periods, arterial development parallels that of the airways. As the fetus matures, the vessels increase in diameter and length, and in the postnatal stage a marked increase in branching occurs, which corresponds to the proliferating alveolar development of early childhood until approximately 8 years of age.

Pulmonary Veins

In the embryonic stage, pulmonary venous blood drains via the splanchnic plexus into the primordium of the systemic venous system, including the cardinal and umbilicovitelline veins (see Fig S3 at *radiographics.rsnajnls.org/cgi/content/full/22/S25/DC1*). Caudal and cranial outpouchings of the sinoatrial regions of the heart develop and extend toward the lung buds. With regression of the caudal portion, the cranial portion continues to develop as the common pulmonary vein, eventually connecting with that portion of the splanchnic plexus draining the lungs. In time, the common pulmonary vein is incorporated into the left atrial wall with obliteration of the majority of the splanchnic pulmonary connections, leaving four independent pulmonary veins directly entering the left atrium.

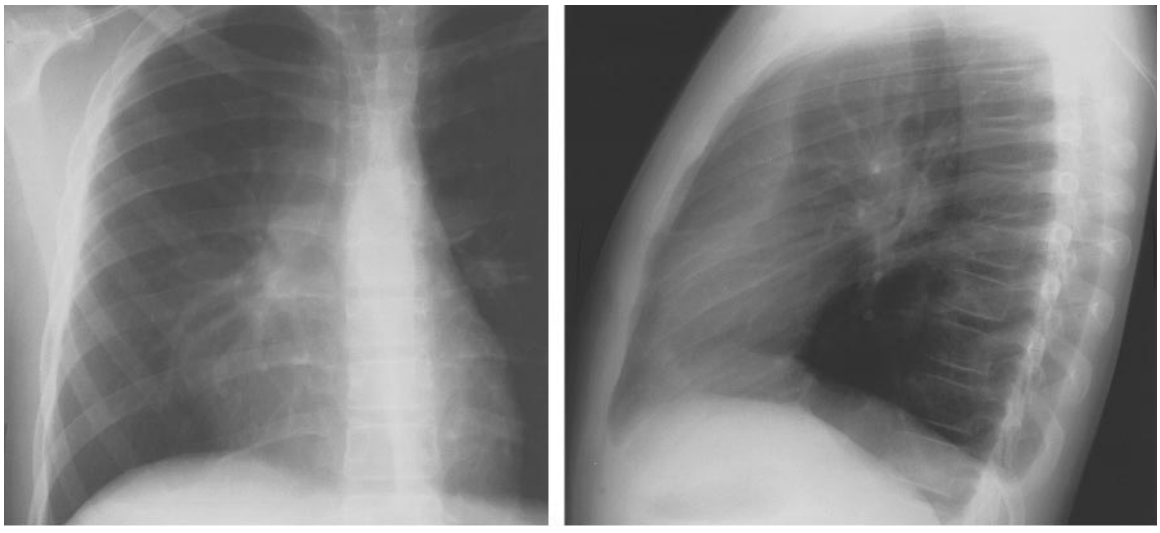

a. b.

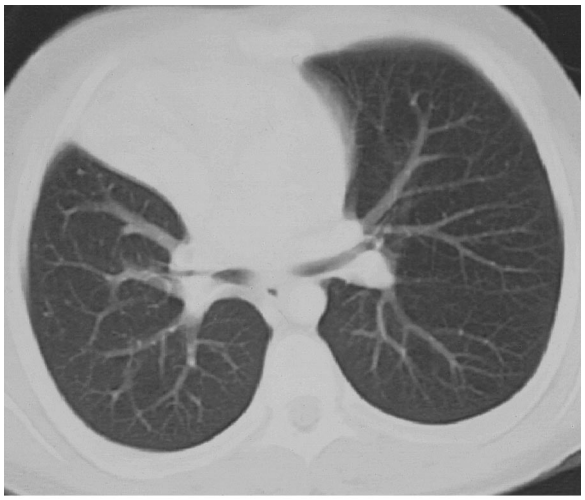

c.

Figure 1. Agenesis of the right upper lobe. **(a, b)** Posteroanterior **(a)** and lateral **(b)** radiographs show a reduction in the volume of the right lung with obscuration of the right border of the heart. An anterior area of increased opacity on the lateral view **(b)** simulates collapse of the right upper and middle lobes. **(c)** Computed tomographic (CT) scan shows absence of the right upper lobe bronchus and shift of the heart to the right. This shift simulates collapse of the right upper and middle lobes and accounts for the anterior area of increased opacity on the lateral radiograph **(b)**. Ventilation and perfusion are otherwise normal.

Bronchopulmonary (Lung Bud) Anomalies

Agenesis

Radiographically, agenesis of a lung simulates a pneumonectomy. The remaining lung is overinflated with accompanying shift of the mediastinum. Agenesis of a lobe (Fig 1) may appear normal or sometimes be confused with collapse of a lobe. Perfusion studies, whether nuclear scanning, angiography, or CT, can readily enable diagnosis.

Cunningham and Mann (1) present eight cases, all of which had associated congenital abnormalities of other systems on the same side as the agenesis. Their literature review identified 71 cases of agenesis associated with other malformations. They hypothesize an abnormality of blood flow in the dorsal aortic arch during the 4th week of gestation.

Congenital Bronchial Atresia

The common sites of involvement in congenital bronchial atresia are the apicoposterior segmental bronchus of the left upper lobe and segmental bronchi of the right upper lobe, middle lobe, and occasionally the lower lobe. Pathogenesis may relate to intrauterine interruption of bronchial arterial blood supply, resulting in ischemia and scarring or discontinuity between the cells at the tip of a bronchial bud with the bud itself. The distal branches can develop normally in the absence of a connection between the distal and central airways.

The radiographic features include a hilar mass and overinflation of the peripheral lung secondary to entrapment of air admitted via collateral air drift. The dilated bronchi contain retained secretions and can have a varied appearance. The branches may simulate horns, as they often taper peripherally. Occasionally, the dilated bronchi are

Figure 2. Bronchial atresia in a 38-year-old man who experienced repeated pulmonary infections. **(a, b)** Frontal radiograph **(a)** and CT scan **(b)** show an appearance suggestive of congenital bronchial atresia. These images accompanied a request for biopsy of a mass in the left upper lobe. The mass contained air and fluid. There was distortion of the lung peripheral to the mass. **(c)** Follow-up posteroanterior radiograph obtained 1 month later shows a decrease in the fluid within the mass. Peripheral linear areas of increased opacity are also present, which likely represent scarring. **(d)** CT scan obtained at the same time as **c** shows distortion of the left upper lobe architecture with linear scarring. The dilated bronchi are air filled or contain air and fluid. A supplying bronchus could not be identified. The patient underwent a left upper lobectomy. **(e)** Photograph of the specimen shows an opened bronchus that communicates with a 4 × 3 × 2-cm cavity, which contained mucus and firm debris. A second cavity 2 cm in diameter was also found. The lingula was not involved.

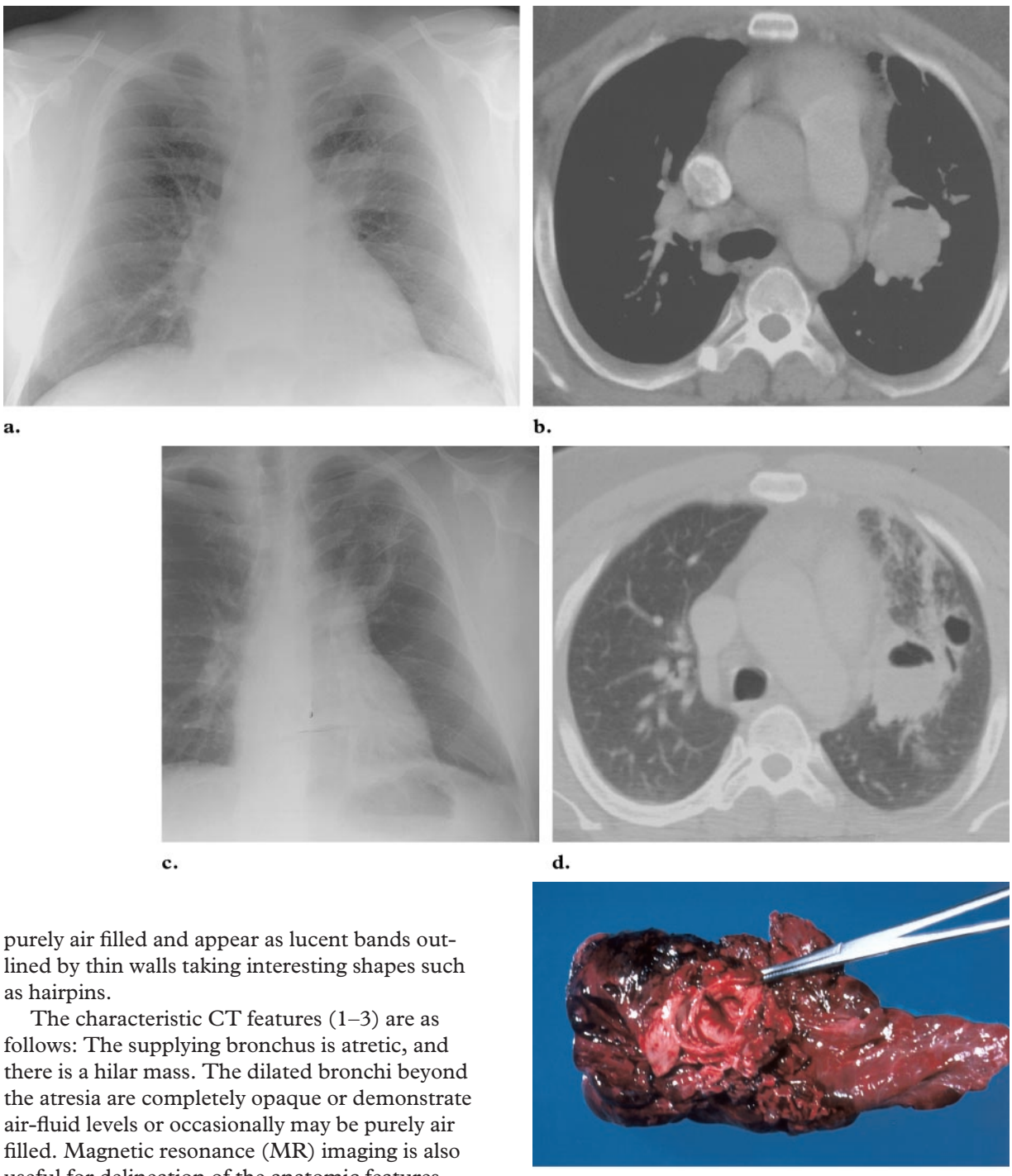

purely air filled and appear as lucent bands outlined by thin walls taking interesting shapes such as hairpins.

The characteristic CT features (1–3) are as follows: The supplying bronchus is atretic, and there is a hilar mass. The dilated bronchi beyond the atresia are completely opaque or demonstrate air-fluid levels or occasionally may be purely air filled. Magnetic resonance (MR) imaging is also useful for delineation of the anatomic features (3). These patients are usually asymptomatic and do not require surgery. The major indication for surgery is repeated infections (Fig 2; see also Figs S4 and S5 at *radiographics.rsnajnls.org/cgi/content/full/22/S25/DC1*).

Mori et al (3) describe an example of atresia of the medial branch of the anterior segmental bron-

Figure 3. Congenital lobar emphysema (overinflation) in a 21-year-old man with sudden onset of shortness of breath and pain in the left anterior part of the chest that was worse during exertion and deep breathing. **(a)** Frontal radiograph shows hyperinflation of the left lower lobe with a paucity of blood vessels. There is a slight shift of the mediastinum to the right. **(b)** CT scan also shows marked overinflation of the left lower lobe. The patient underwent a left lower lobectomy. At gross examination, the bronchi were extremely thin and poorly developed. **(c)** Photomicrograph (original magnification, ×2.5; hematoxylin-eosin stain) shows hyperaerated lung parenchyma with distended or hyperinflated alveoli and alveolar ducts. **(d)** Photomicrograph (original magnification, ×7; hematoxylin-eosin stain) of a cross section of the bronchial tree shows thin, underdeveloped, immature-appearing cartilage plates (arrowhead).

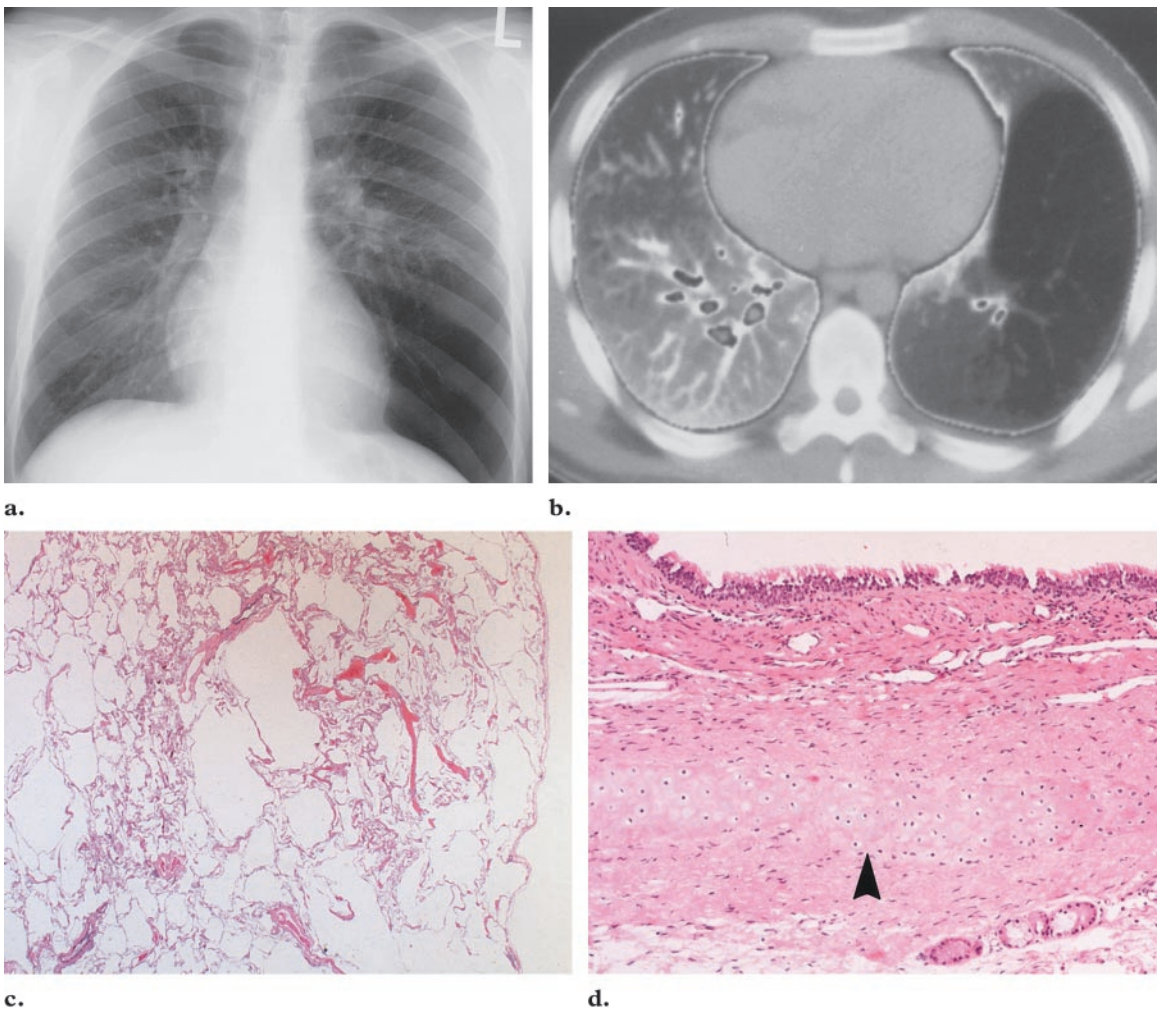

chus of the right upper lobe with the classic features of a hilar mass and peripheral hyperlucency. CT and MR imaging allow confirmation of the diagnosis and, in the absence of complications such as infection, enable postponement of surgery.

Congenital Lobar Emphysema

Congenital lobar emphysema or hyperinflation is usually diagnosed in the neonatal period or infancy. It is more common in males than females (3:1). The left upper lobe and right middle lobe are the usual sites, with the lower lobes rarely being affected. There is controversy as to whether the condition is developmental or acquired. Deficiency of cartilage would suggest a developmental cause. The radiographic features are those of overinflation with air trapping on expiration (Fig 3).

On extensive review of the literature, Murray (4) concluded that lobar emphysema could be congenital or acquired and that many conditions causing bronchial obstruction could be causative, including congenitally defective cartilage and acquired bronchial mucous plugs. Kennedy et al (5) followed conservatively treated cases for several months and concluded that the condition was improving.

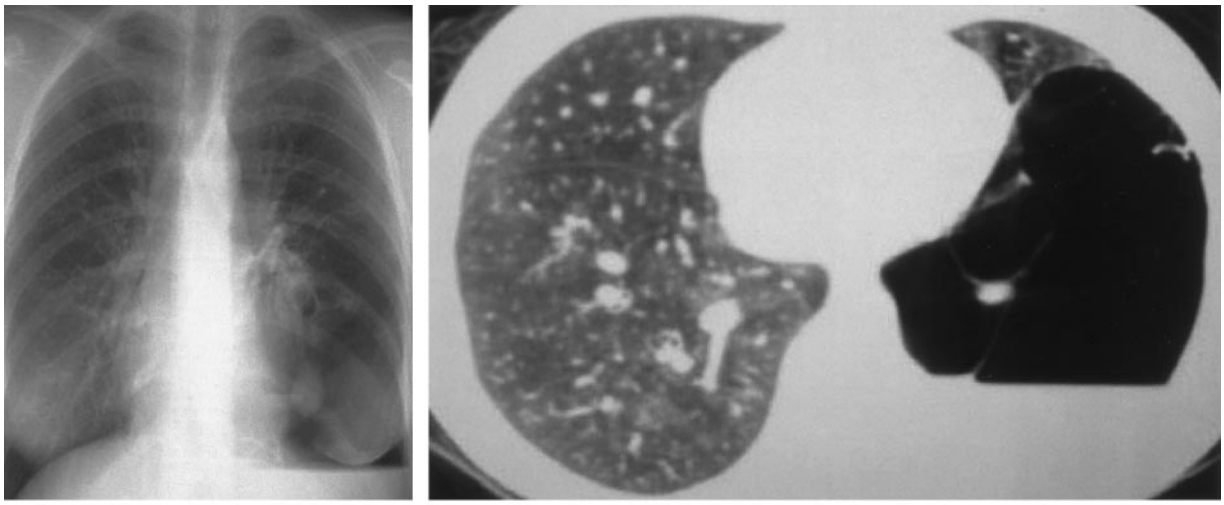

a. b.

Figure 4. Congenital cystic adenomatoid malformation in a 31-year-old woman with a history of recurrent pneumonia. **(a)** Frontal radiograph shows a long air-fluid interface and a large rounded area of increased opacity that dips into the air. Medially, there is a second air-fluid interface and a small oval area of increased opacity. The volume of the left lung is increased with shift of the mediastinum to the right. **(b)** CT scan shows thin-walled spaces containing air and fluid in the basal segments of the left lower lobe. At the time of the frontal radiography study, the largest cyst contained air and fluid, whereas the two opaque cysts were filled with fluid. The diagnosis was confirmed at surgery. The specimen demonstrated an expansile, septated cystic mass. (Courtesy of N. L. Müller, MD, Vancouver Hospital, Vancouver, Canada.)

Congenital Cystic Adenomatoid Malformation

Congenital cystic adenomatoid malformation is said to account for 25% of all congenital lung abnormalities. The lesion consists of adenomatoid proliferation of bronchioles that form cysts instead of normal alveoli. Three types have been classified by pathologic analysis. Type I consists of cysts measuring 2–10 cm and is the most common variety. Type II has numerous smaller, more uniform cysts measuring 0.5–2 cm in diameter, and type III are solid-appearing lesions that microscopically demonstrate tiny cysts.

Although it is usually unilateral, Plit et al (6) report a case of bilateral congenital cystic adenomatoid malformation. The anomaly has been described within a sequestration by Zangwill and Stocker (7), in association with extralobar intra-abdominal sequestration by Fraggetta et al (8), and in association with sequestration by Conran and Stocker (9). Hellmuth et al (10) describe an example of congenital cystic adenomatoid malformation manifesting as unilobar cysts. The CT findings in seven cases are reported by Patz et al (11). Six patients were subject to recurrent pneumonia and one to recurrent pneumothorax. CT features consisted principally of a complex cystic mass in addition to the pneumonias. In their review of congenital lesions that may mimic neoplasms in adults, Raymond et al (12) describe a circumscribed conglomeration of multiple cysts in a lower lobe, an appearance difficult to distinguish from sequestration.

The disorder is usually diagnosed in the neonatal period and the first 2 years of life. It is rarely encountered in the adult. In the adult, the lower lobes are usually involved, with expansion of the involved hemithorax and compensatory shift of the mediastinum. The cysts may be single or multiple, containing air, fluid, or both (Fig 4; see also Fig S6 at *radiographics.rsnajnls.org/cgi/content/full/22/S25/DC1*).

Pulmonary Bronchogenic Cysts

Bronchogenic cysts are thought to result from abnormal budding of the developing tracheobronchial tree with separation of the buds from the normal airways. Sixty-five percent to 90% of bronchogenic cysts are mediastinal. When they are pulmonary, they are usually solitary, thin walled, and unilocular. Infection is frequent. The common location is the lower lobes (Fig 5).

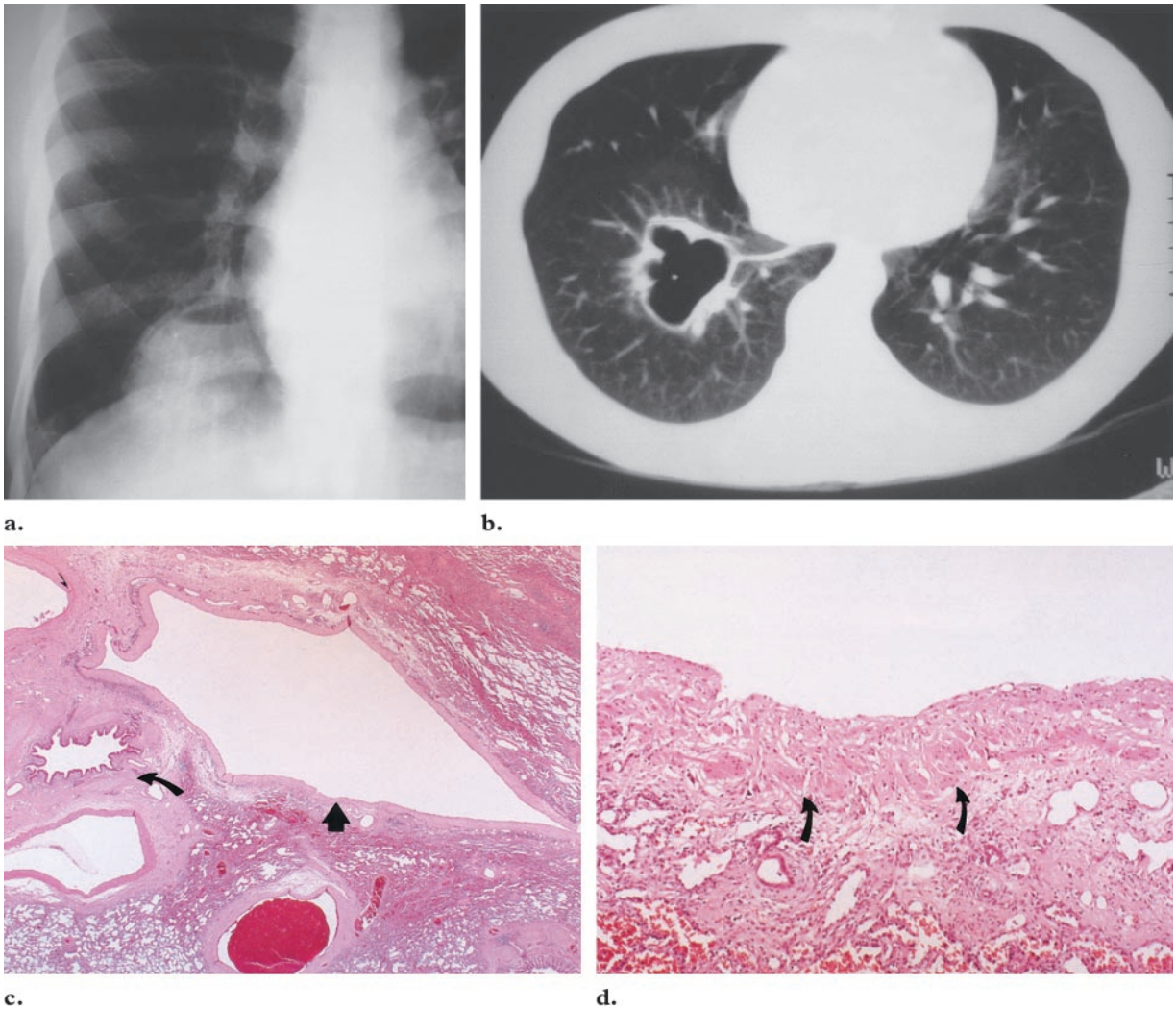

Figure 5. Pulmonary bronchogenic cyst in a 15-year-old boy with right lower lobe pneumonia. **(a)** Frontal radiograph shows a well-defined lesion with an air-fluid level near the superior margin of the right lower lobe. **(b)** CT scan shows the air-containing space and its well-defined wall. The lesion was resected. **(c)** Photomicrograph (original magnification, ×2.5; hematoxylin-eosin stain) shows an intrapulmonary cystically dilated space (straight arrow) adjacent to the bronchovascular tree (curved arrow). **(d)** Photomicrograph (original magnification, ×25; hematoxylin-eosin stain) of the cyst wall shows no epithelial lining. The presence of discontinuous, discrete smooth muscle bundles in the cyst wall (arrows) suggests a bronchogenic origin for the cyst.

Bronchogenic cysts may be first detected as incidental findings on radiographs obtained for some other purpose or they may signal their presence because of infection or compression phenomena. The literature contains much writing by surgeons (13) who have removed the lesion from a number of symptomatic patients and who sometimes suggest that all of these lesions should be removed. Aktogu et al (13) analyzed 31 cases of bronchogenic cyst, of which only six were asymptomatic. In conjunction with their review of the literature, they discuss the fact that bronchogenic cysts are frequently asymptomatic and are an incidental finding in a radiograph obtained for some other purpose. Although these authors are surgically oriented and hold to the view that these lesions should be resected because they will in time become symptomatic, they point out that there is no series with long-term follow-up of asymptomatic bronchogenic cysts to support a conservative approach.

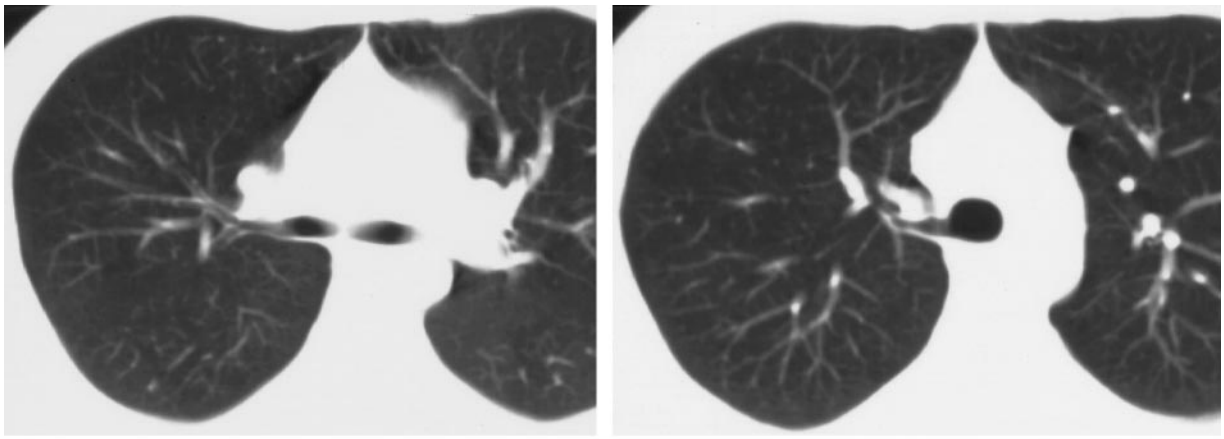

a. b.

Figure 6. Displaced tracheal bronchus. **(a)** CT scan shows that the right upper lobe bronchus bifurcates. **(b)** CT scan shows that the apical bronchus originates from the trachea.

Tracheal Bronchus

A tracheal or pig bronchus arises from the trachea superior to the carina (Fig 6). It is probably secondary to an additional tracheal outgrowth early in embryonic life. It occurs almost exclusively on the right and usually within 2 cm of the carina. The bronchus is supernumerary if the right upper lobe bronchus trifurcates normally. It is displaced if the right upper lobe bronchus bifurcates. The displaced bronchus usually supplies the apical segment.

As might be expected, the tracheal bronchus is subject to disease. Patrinou et al (14) report a case of carcinoid tumor of a tracheal bronchus.

Accessory Cardiac Bronchus

The accessory cardiac bronchus most commonly arises from the inferior medial wall of the right main or intermediate bronchus (Fig 7). It may end blindly or be associated with small amounts of abnormal pulmonary parenchyma. The accessory bronchus may serve as a potential reservoir of infectious organisms with resultant hemorrhage, cough, or recurrent pneumonia.

McGuinness et al (15) report six cases. One resected specimen included some abnormal lung tissue but normal endobronchial mucosa and cartilage in the wall of the bronchus. In four cases,

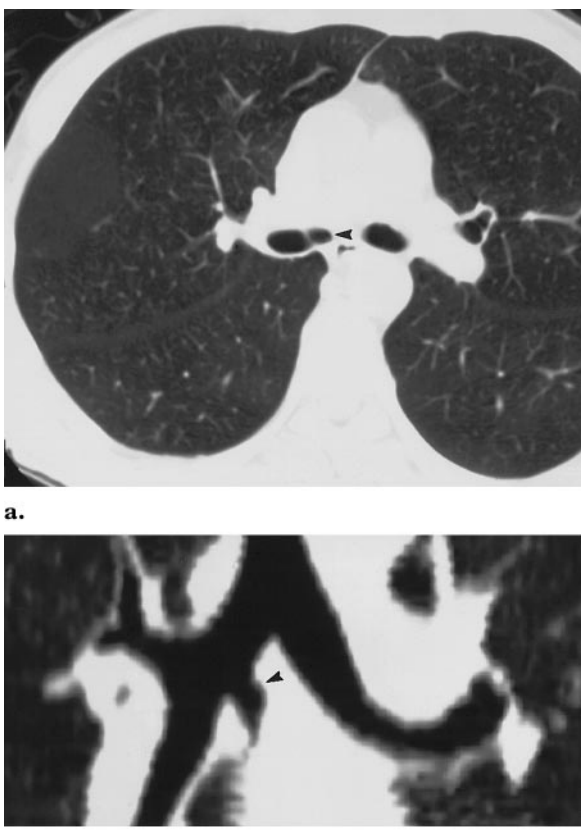

a. b.

Figure 7. Accessory cardiac bronchus. Axial CT scan **(a)** and coronal reformatted image **(b)** show an accessory cardiac bronchus (arrowhead) that originates from the medial aspect of the right main bronchus. (Case courtesy of the Department of Radiology, University of Michigan, Ann Arbor.)

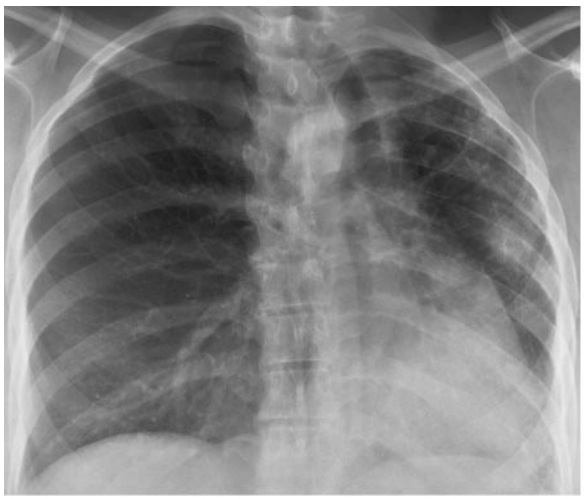

a.

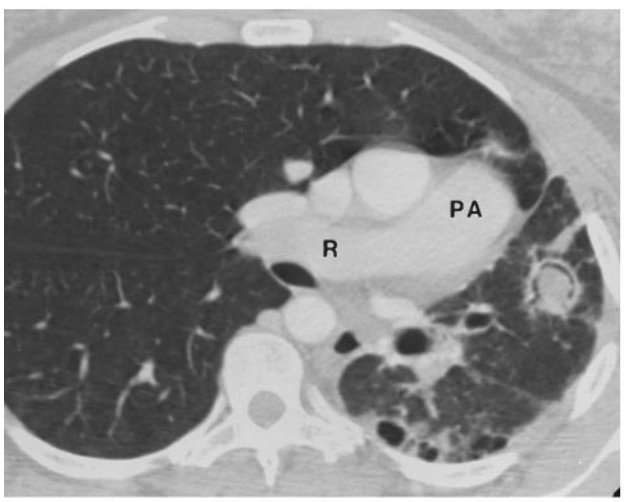

b.

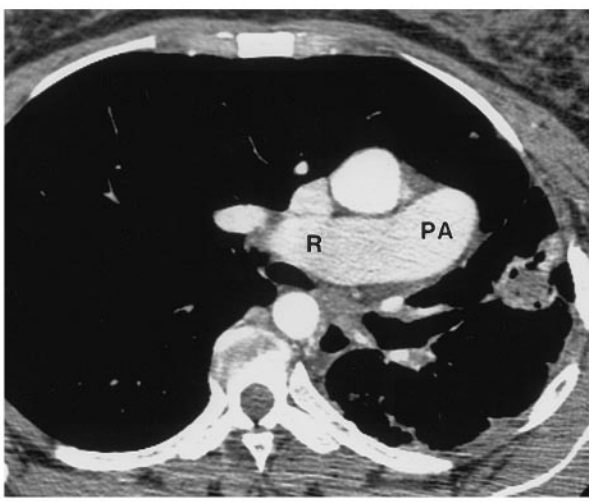

c.

Figure 8. Congenital absence of the left pulmonary artery in a 46-year-old woman with an incorrect diagnosis of Swyer-James syndrome since 1987. **(a)** Frontal radiograph shows a right aortic arch and shift of the mediastinum to the left. The white line that parallels the medial aspect of the left scapula represents the displaced anterior junction line. The round area of increased opacity in the left middle lung zone had been stable for several years. **(b, c)** CT scans show absence of the left pulmonary artery. The area of increased attenuation in the left middle lung zone represents a cavity with material within it, which was presumed to be a fungus ball. There are also small areas of decreased attenuation in the periphery of the left lung, which represent paraseptal emphysema. *PA* = main pulmonary artery, *R* = right pulmonary artery.

CT showed an apparent pleural fissure delimiting the lung tissue. These authors raise the question of whether this is really an accessory lobe.

Vascular Anomalies

Interruption (Absence) of a Main Pulmonary Artery

In interruption of a main pulmonary artery, right-sided involvement is more common than left-sided involvement. The affected lung is decreased in size, as is the hilum. The diminutive vessels are systemic. Therefore, the lung is hyperlucent. However, there is no evidence of air trapping on expiration, as in the Swyer-James syndrome. Ventilation-perfusion lung scans demonstrate ventilation with no perfusion, whereas in the Swyer-James syndrome there is reduction in both ventilation and perfusion. Interruption of the left pulmonary artery is much less common and may be associated with congenital cardiovascular anomalies (Fig 8; see also Figs S7 and S8 at *radiographics.rsnajnls.org/cgi/content/full/22/S25/DC1*).

In the absence of a pulmonary arterial supply, Ellis (16) describes the bronchial arteries, a patent ductus, major aortopulmonary collateral arteries, direct origin of a pulmonary artery from the aorta, and other systemic arteries supplying the lung. Coronary-to–left pulmonary artery anastomoses are also noted. Bouros et al (17) report six male patients, aged 17–20 years, who were found to have unilateral pulmonary artery agenesis at preinduction military screening. Two of the four patients who underwent bronchography were found to have bronchiectasis; three had right aortic arch; one had transposition of the great vessels; and one had a truncus. The diagnoses were confirmed with MR imaging. Gotway et al (18) illustrate absence of the left pulmonary artery, which was an incidental finding.

Anomalous Origin of the Left Pulmonary Artery from the Right

Anomalous origin of the left pulmonary artery from the right is usually diagnosed in infancy because of the effect of the aberrant artery on the

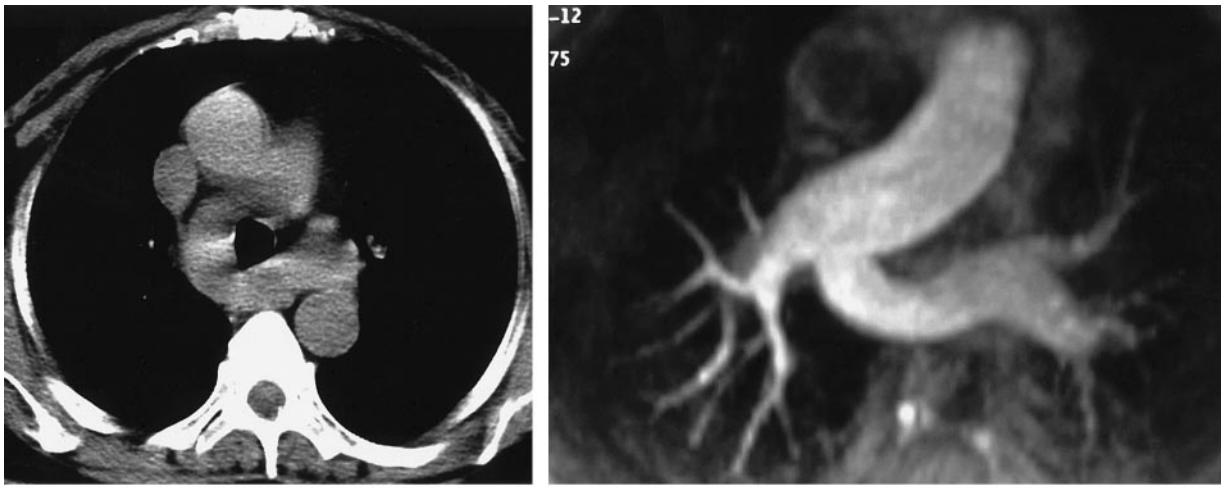

a. b.

Figure 9. Anomalous origin of the left pulmonary artery from the right in an asymptomatic adult. CT scan **(a)** and MR angiogram **(b)** show the course of an anomalous left pulmonary artery. Originating from the posterior surface of the right pulmonary artery, it passes posteriorly adjacent to the trachea and turns to the left to enter the left hilum. (Case courtesy of Eva Castaner, MD, Hospital Parc Jauli, Sabadell, Spain.)

airway and often the associated tracheal or bronchial stenosis due to complete cartilage rings. This can result in obstruction, feeding problems, and respiratory tract infections (19). Occasionally, the abnormality may be detected as an incidental finding in an asymptomatic adult (Fig 9) or in the adult with respiratory complaints. The aberrant left pulmonary artery originates from the right pulmonary artery and travels posteriorly to the right of the distal trachea or right main bronchus, where it turns abruptly to the left, passing between the esophagus and trachea to its destination in the left hilum. This anomalous artery has been called a *sling*. The anomalous pulmonary artery may be accompanied by tracheobronchial stenosis resulting from complete cartilaginous rings—a life-threatening feature in infants called the *ring-sling complex*.

Although more commonly discovered during childhood, pulmonary sling may be identified in symptomatic or asymptomatic adults. Hatten et al (20) report an asymptomatic 45-year-old man whose sling was an incidental finding on a chest radiograph obtained for other indications. The aberrant left pulmonary artery was depicted as a right paratracheal mediastinal mass. A lateral examination showed a mass between the distal trachea and esophagus; barium filling of the esophagus outlined the pressure deformity of the anterior esophageal contour. Pickhardt (21) reports a 19-year-old patient with sickle cell disease who, when studied with ventilation-perfusion scans of the lung because of chest pain, revealed global hypoperfusion of the left lung in the presence of normal ventilation. CT and angiography clarified the diagnosis of pulmonary sling. Malmgren et al (22) report one adult and two children with pulmonary sling who were examined with radiography, barium esophagography, angiography, and MR imaging. The MR imaging was considered diagnostic by itself. The usefulness of MR imaging in making the diagnosis is stressed by Malmgren et al (22). Lin et al (23) report the combination of agenesis of the right lung and sling. Koch et al (24) report a patient with both an anomalous and a small conventional left pulmonary artery. This combination is also recorded (in an infant) by Ge et al (25). Although adults with sling rarely have complete tracheal rings, a life-threatening associated anomaly in children, such a case is documented by Lee et al (26). The left pulmonary artery has been surgically reimplanted by using cardiopulmonary bypass in a number of cases.

Anomalous Pulmonary Venous Drainage

Anomalous pulmonary venous drainage results in an extracardiac left-to-right shunt as pulmonary venous blood flows directly into the right side of the heart or systemic veins. It may be partial or

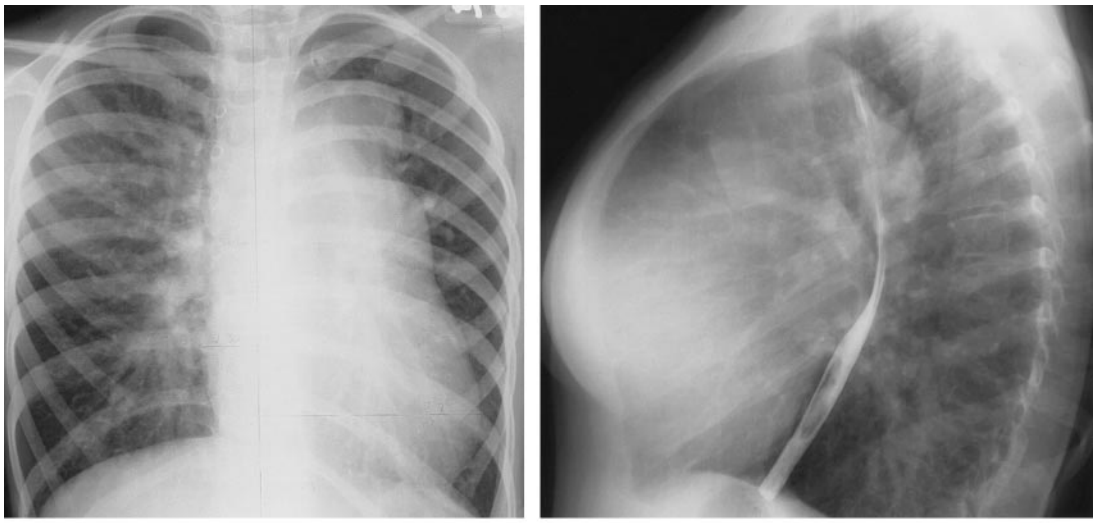

a. b.

Figure 10. Total anomalous pulmonary venous return in a young woman with a patent ductus arteriosus. **(a)** Anteroposterior radiograph shows that the mediastinum is widened, particularly on the left side, where there is a communication with the left brachiocephalic vein. The changes on the right side are minimal. Increased arterial flow is readily apparent. **(b)** Left lateral radiograph shows a large high aortic arch, enlargement of the right cardiac chambers, and overfilled pulmonary arteries.

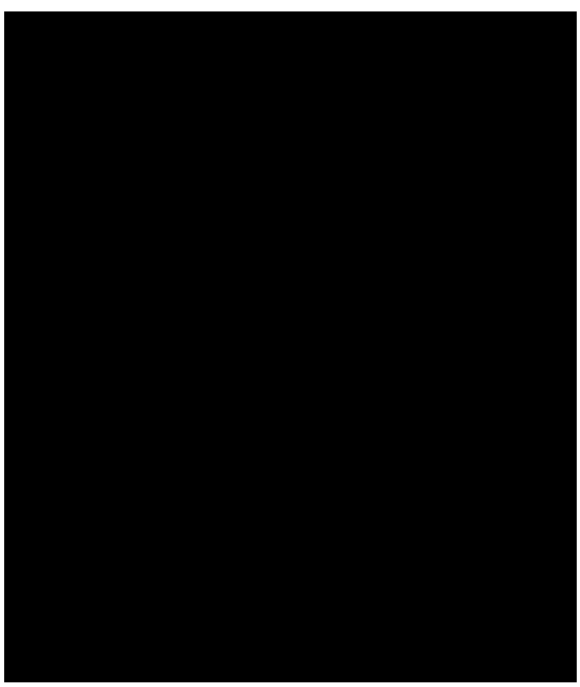

Figure 11. Diagram shows types of total anomalous pulmonary venous return. *CPV* = common pulmonary vein, *CS* = coronary sinus, *IVC* = inferior vena cava, *LA* = left atrium, *LPV* = left pulmonary vein, *LV* = left ventricle, *PVS* = portal venous system, *RA* = right atrium, *RPV* = right pulmonary vein, *RV* = right ventricle. (Adapted and reprinted, with permission, from reference 51.)

total, the latter requiring a right-to-left shunt via a cardiac septal defect or patent ductus arteriosus (Fig 10). The anomalous connections have been classified into four groups: supracardiac, cardiac, infradiaphragmatic, and mixed (Fig 11). The likely explanation is failure of connection between the primitive pulmonary splanchnic plexus and the common pulmonary vein derived from the atrium. An anomalous vein on occasion has been found on conventional radiographs. It is recognized with increasing frequency at CT and is perhaps more common than previously thought.

Adler and Silverman (27) present three cases of partial anomalous drainage of the left upper lobe with both radiographic and CT demonstration. In their cases, a vertical vein drained to the left brachiocephalic vein. A right superior pulmonary vein draining to the azygos vein is documented by Thorsen et al (28). Dillon and Camputaro (29) found radiographs of no help in distinguishing persistent left superior vena cava on its way to the coronary sinus from anomalous pulmonary venous drainage of the left upper lobe. Careful analysis of CT scans is required; two vessels are seen anterior to the left main bronchus in

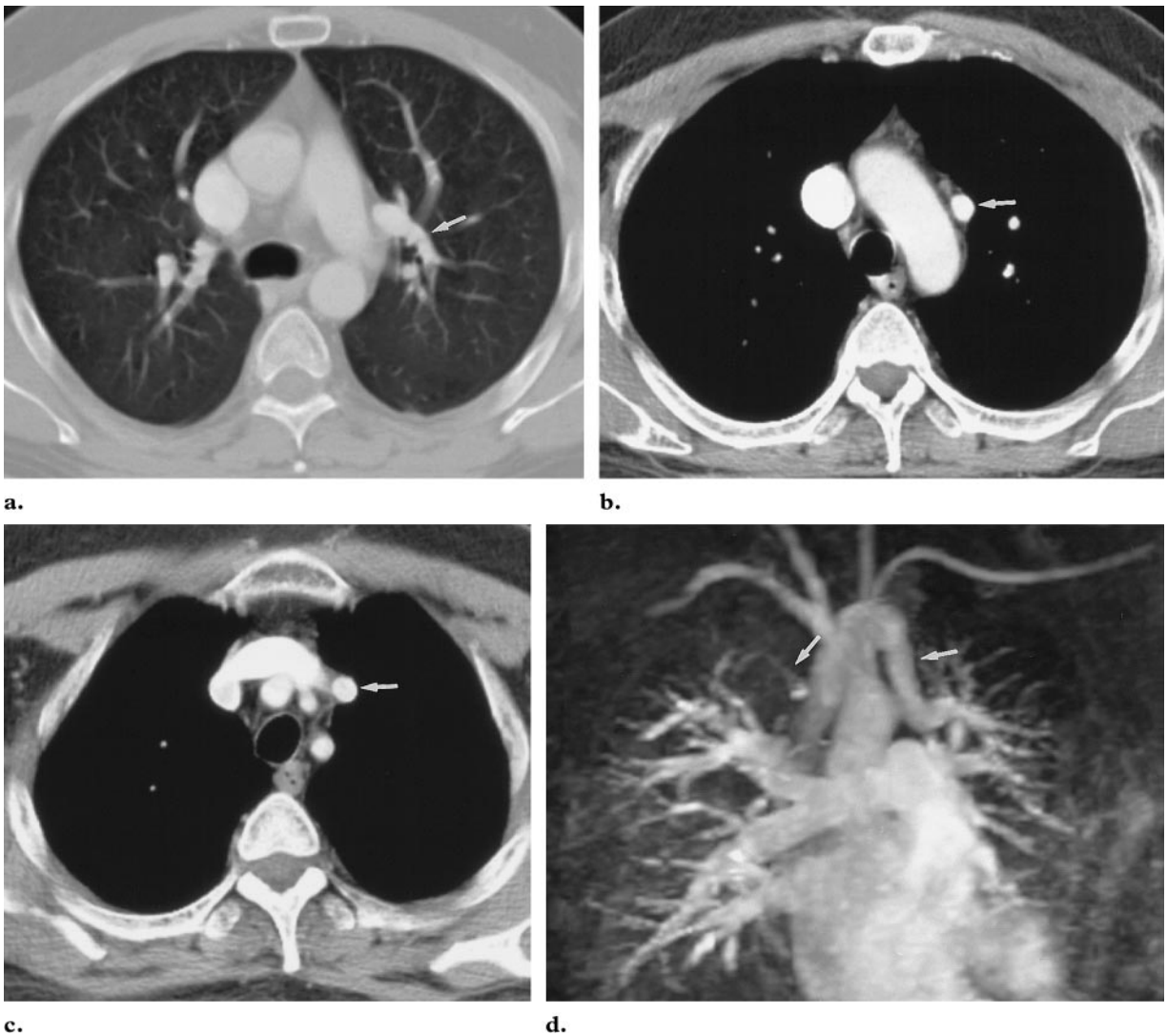

Figure 12. Anomalous pulmonary vein from the left upper lobe in a 54-year-old man. **(a–c)** CT scans show drainage of an anomalous left upper lobe vein (arrow) into the left brachiocephalic vein. Distinction from a left superior vena cava is made with CT (see text). **(d)** Coronal MR angiogram of another patient shows anomalous drainage of a left upper lobe vein into the left brachiocephalic vein (right arrow) and partial drainage of the right upper lobe into the superior vena cava (left arrow). (Fig 12d courtesy of C. Higgins, MD, University of California, San Francisco.)

persistent left superior vena cava, whereas none are there with anomalous left upper lobe venous drainage. Gilkeson et al (30) illustrate an anomalous left inferior pulmonary vein joining the left upper pulmonary vein, which then empties to the left atrium. Viamonte (31) illustrates an inferior right pulmonary vein draining the entire right lung to the right atrium; perhaps this should be designated a "super-scimitar."

Examples of anomalous drainage of the upper lobes are shown in Figures 12 and 13 (see also Fig S9 at *radiographics.rsnajnls.org/cgi/content/full/22/S25/DC1*).

Pulmonary Arteriovenous Malformation

Pulmonary arteriovenous malformation can occur in isolation, be multiple, or be part of a systemic process where arteriovenous communications occur in the skin, mucous membranes, and other organs (hereditary hemorrhagic telangiectasia or Rendu-Osler-Weber disease). Swanson et al (32) record their extensive experience. The lesions tend to be recognized with increasing age, as time is required for the effects of the flow to become manifest (Fig 14).

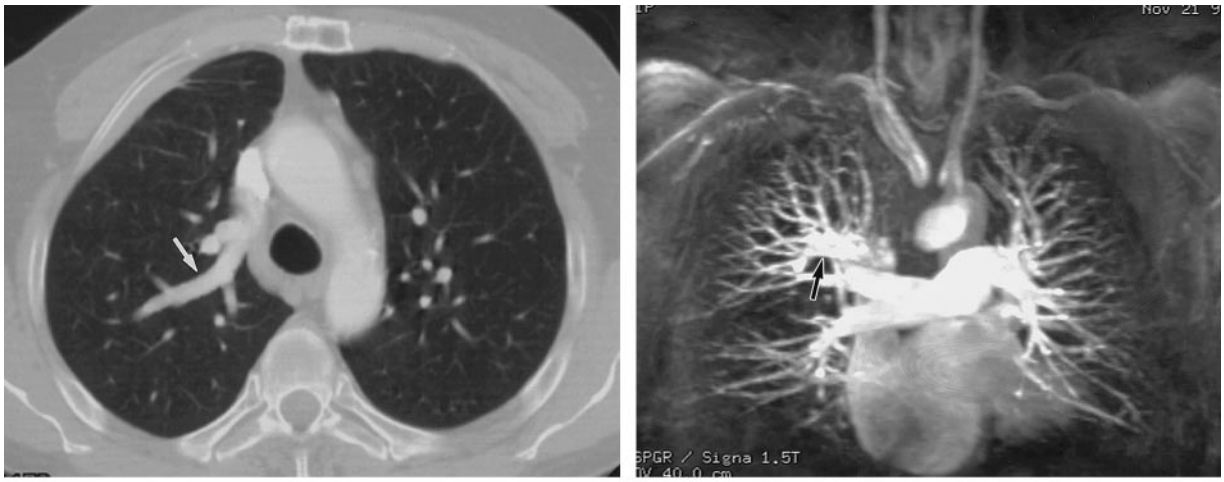

a. b.

Figure 13. Anomalous pulmonary vein from the right upper lobe in a 69-year-old man. **(a)** CT scan shows a connection from an anomalous right upper lobe vein (arrow) to the superior vena cava. **(b)** Coronal MR angiogram of another patient shows anomalous drainage of a right upper lobe vein into the superior vena cava (arrow). (Fig 13b courtesy of C. Higgins, MD.)

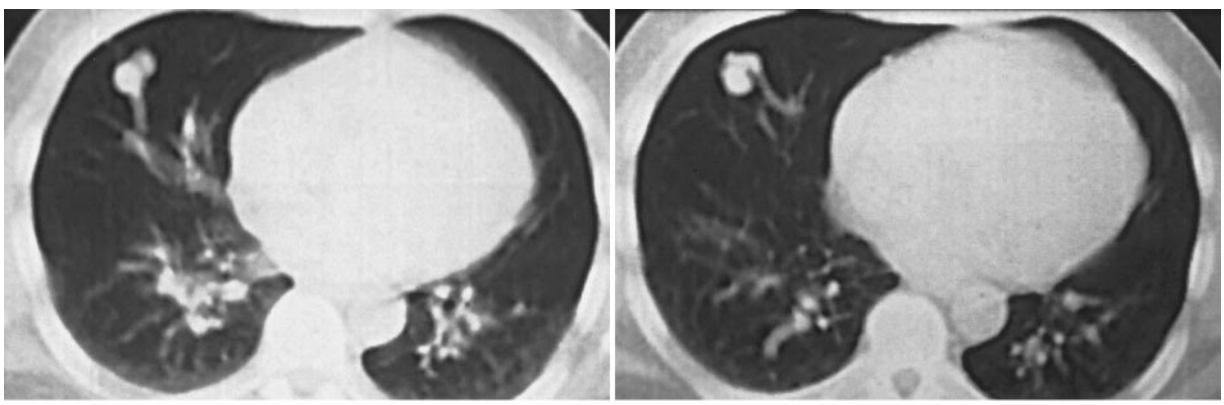

b.

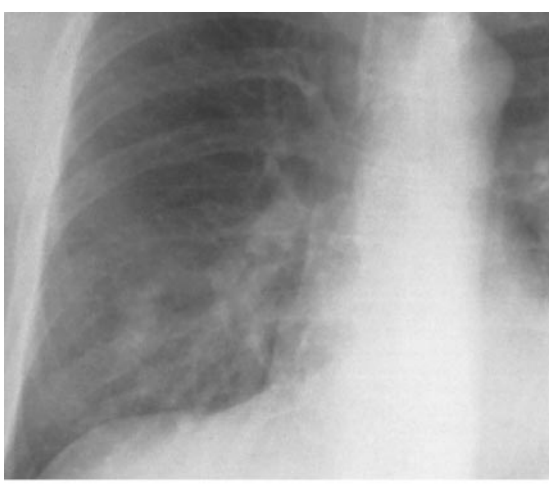

a.

Figure 14. Arteriovenous malformation. **(a)** Frontal radiograph shows a nodular area of increased opacity in the right middle lobe. **(b)** CT scans show an arteriovenous malformation. The supplying and draining vessels are clearly seen. The lateral segment of the right middle lobe and the lingula are the most common locations for a solitary arteriovenous malformation. (Case courtesy of J. Wandtke, MD, University of Rochester, Rochester, NY.)

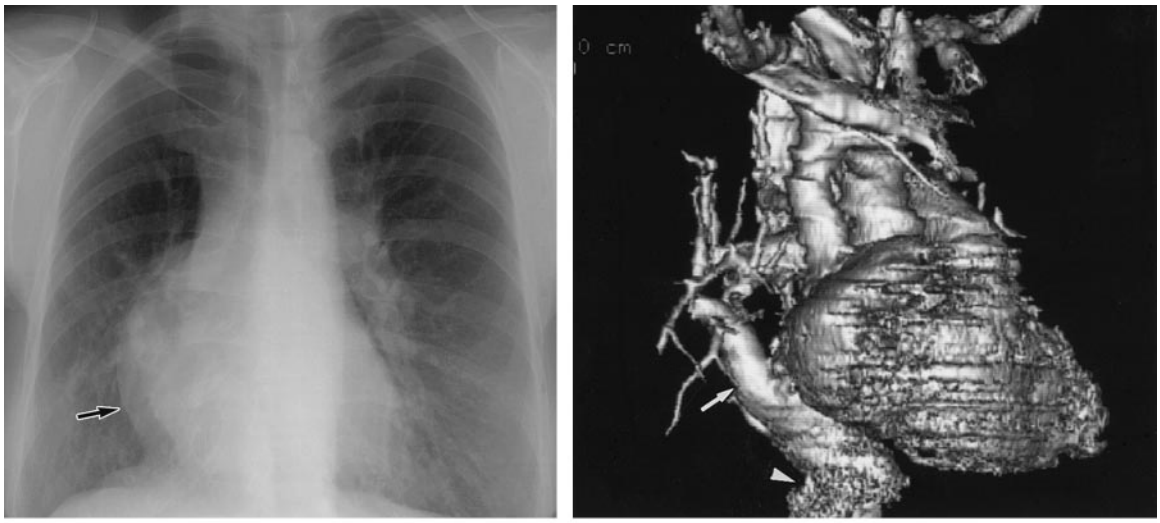

a. b.

Figure 15. Hypogenetic lung (scimitar) syndrome in a 68-year-old asymptomatic woman who underwent a routine preoperative study. **(a)** Frontal radiograph shows shift of the mediastinum to the right secondary to volume loss. The patient does not have a right upper lobe. The right hilum appears small; however, the pulmonary artery was of normal size on CT scans. An oblong area of increased opacity (arrow) parallels the right border of the heart. **(b)** Volume-rendered CT image shows the oblong area of increased attenuation (arrow) parallel to the right border of the heart. This finding represents an anomalous vein that drains into the inferior vena cava (arrowhead).

Combined Lung and Vascular Anomalies

Hypogenetic Lung (Scimitar) Syndrome

Hypogenetic lung (scimitar) syndrome consists of abnormal development of the lung, which almost always occurs on the right side. The lung is small and associated with a small or absent pulmonary artery and systemic arterial supply. Anomalous venous return is usually into the inferior vena cava below the right hemidiaphragm, although it may join with the suprahepatic portion of the inferior vena cava, hepatic vein, portal vein, azygos vein, coronary sinus, or right atrium. Associated pulmonary abnormalities include anomalies of the right bronchial tree, which is commonly a mirror image of the left, and diverticula. Accompanying cardiovascular anomalies are frequent.

Conventional radiographic findings are often diagnostic, particularly with the anomalous draining vein forming the familiar curvilinear tubular area of increased opacity (scimitar) heading in the direction of the inferior vena cava. The affected lung is small and hyperlucent. Pulmonary vessels do not have a normal arrangement, as they may be systemic. The unaffected lung is hyperinflated with resultant shift of the mediastinum to the affected side. An illustrative case is shown in Figure 15. Additional information can be obtained with conventional tomography, CT, and MR imaging. There are many variations on the usual themes, as detailed by Woodring et al (33) in a general review. They suggest that the most common components of congenital pulmonary venolobar syndrome are hypogenetic lung and anomalous pulmonary venous return. Reports of isolated anomalous systemic supply to the lower lobes without bronchial abnormality are made by Ko et al (34) among others.

Bronchopulmonary Sequestration

Bronchopulmonary sequestration, intralobar and extralobar, represents an anomaly of tracheobronchial branching with retention of the embryonic

Comparison of Various Features of Intralobar and Extralobar Sequestrations

Feature	Intralobar Sequestration	Extralobar Sequestration
Relative prevalence	6:1	1:6
Age at diagnosis	Adult	Neonate (related to CHD*)
Sex distribution	Equal	80% male
Location	60% left base, 40% right base	90% left side in association with the left hemidiaphragm; 80% associated with posterior congenital diaphragmatic hernia
Pleura	Visceral pleura around lung	. . .
Arterial supply	Systemic; usually a single large artery from the thoracic or abdominal aorta	Systemic; small artery from the aorta
Drainage	Pulmonary veins	Systemic; azygos or hemiazygos system
Pulmonary artery supply	Absent	May be present
Bronchi	Rare	May connect to gastrointestinal tract
Association with congenital anomalies	Rare	Common

Note.—Infection may occur with intralobar sequestration. It is rare with extralobar sequestration, as such a sequestration is enveloped by its own visceral pleura.
*CHD = congenital heart disease.

systemic arterial supply. Details are provided in the Table.

The prevalence of sequestration is the highest among the conditions considered in this review. Although many are found incidentally at radiography of the chest, massive hemoptysis has been reported by Miller et al (35), whereas more commonly recurrent infections as described by Louie et al (36) have led to discovery. The congenital origin of intralobar sequestration is accepted by most, but an acquired origin of intralobar sequestration has been postulated by Stocker (37), Eustace et al (38), and Uppal et al (39). The case reported by Uppal et al (39) had a mycetoma within the sequestration; the systemic supply was from the inferior phrenic artery. Cerruti et al (40) report bilateral lower lobe intralobar sequestrations with horseshoe lung. The systemic supply to the lesion is commonly from a separate branch from the aorta, but upper abdominal vessels and even coronary arteries are described as sources by Hilton et al (41). Hekelaar et al (42) report the case of a 31-year-old nonsmoking patient with left lower lobe sequestration who was found at surgery to have an associated carcinoma of lymphoepithelial type. The use of CT in adult sequestration and other anomalies is reviewed by Rappaport et al (43). MR imaging has been used in three-dimensional contrast material–enhanced mode to characterize sequestration by Au et al (44).

At radiography, intralobar sequestrations can manifest as an area of increased opacity simulating pneumonia, as a mass with or without air-fluid levels, or as cysts. The lower lobes are the most common site, particularly the left, but Gupta et al (45) report two cases of upper lobe sequestration in adults, whereas Hoeffel and Bernard (46) supply an example in a child. The supplying systemic artery is occasionally evident on plain radiographs and is frequently seen at CT. With repeated infections, communication with the bronchial tree may develop. Abnormality of

Figure 16. Sequestration in a 37-year-old woman with a productive cough. **(a, b)** Conventional radiographs show an area of increased opacity in the left lower lobe. **(c)** CT scan shows a vessel that arises from the aorta and supplies the sequestered lung tissue. **(d)** Photomicrograph (original magnification, ×7; hematoxylin-eosin stain) shows a dilated bronchiole with a mucous plug (straight arrow); the injury pattern of bronchiolitis obliterans–organizing pneumonia and fibrosis are seen in the surrounding lung parenchyma (curved arrow). **(e)** Photomicrograph (original magnification, ×20; hematoxylin-eosin stain) shows the wall of the systemic artery (straight arrow) with an adjacent bronchus (curved arrow).

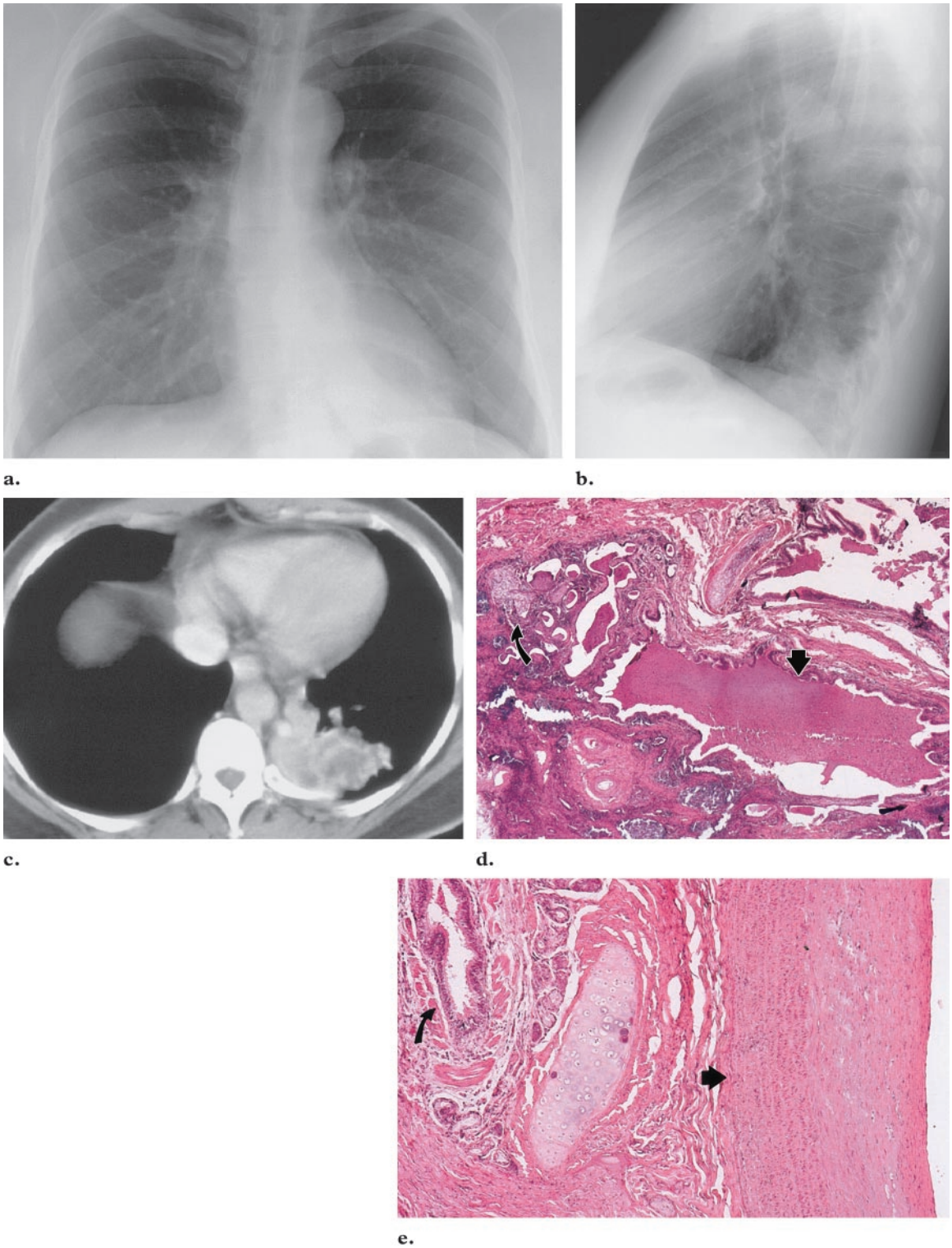

Figure 17. Right intralobar sequestration and left extralobar sequestration in an 18-year-old woman with a history of repeated infections of the right lung. Frontal **(a)** and lateral **(b)** radiographs show extensive abnormality in the right lower lobe. The abnormality consists of cavitation, as evidenced by an air-fluid level. There is some increased opacity in the adjacent parenchyma, which may be due to pneumonia. There is abnormal increased opacity behind the heart medially. The left hemidiaphragm appears to join a posteromedial mass: an extralobar sequestration. (Case courtesy of G. Barnes, MD, Tucson, Ariz.)

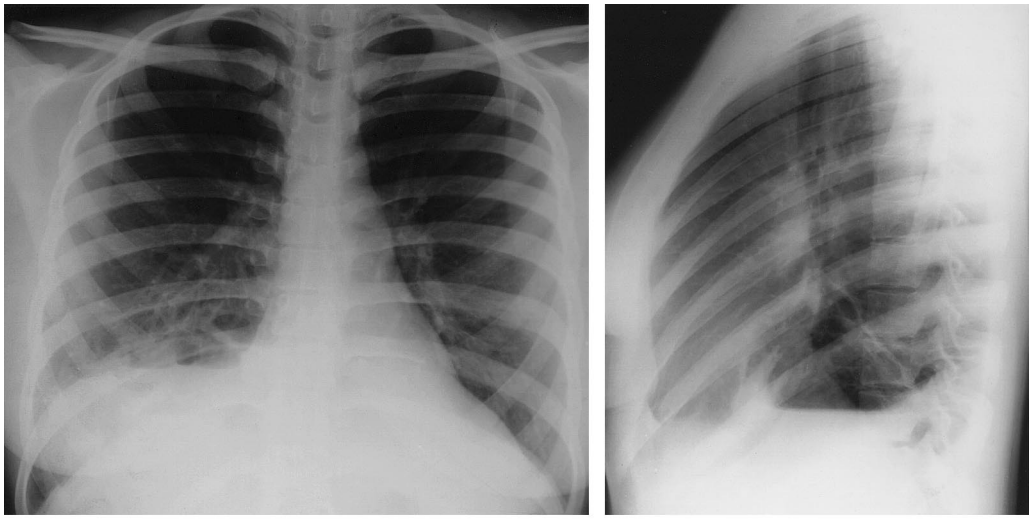

a. **b.**

the lung adjacent to the sequestration is particularly well shown on CT scans. This consists of localized overinflation, likely representing air trapping rather than emphysema. An illustrative case is shown in Figure 16 (see also Figs S10 and S11 at *radiographics.rsnajnls.org/cgi/content/full/22/S25/DC1*).

Extralobar sequestration, in which the sequestered lung has its own separate pleural covering, is much less common and usually is found on the left side next to the hemidiaphragm. At radiography, it may manifest as a reasonably well-defined mass at the base of the left hemithorax. Rarely, an intralobar and extralobar sequestration may occur in the same patient (Fig 17). Extralobar sequestration manifested as a mediastinal mass in the case reported by Ke et al (47). Extralobar sequestration outside of the pleural cavity has been described in the diaphragmatic crus (48) or even in the abdominal cavity or retroperitoneal space, simulating an adrenal mass (49). Rosado-de-Christenson et al (50) review the subject and offer correlation with pathologic features.

Conclusion

This overview has highlighted many of the characteristic imaging features of pulmonary developmental anomalies encountered in the adult. These features may aid in the differentiation from more sinister abnormalities.

References

1. Cunningham ML, Mann N. Pulmonary agenesis: a predictor of ipsilateral malformations. Am J Med Genet 1997; 70:391–398.
2. Mata JM, Caceres J, Lucaya J, Garcia-Conesa JA. CT of congenital malformations of the lung. RadioGraphics 1990; 10:651–674.
3. Mori M, Kidogawa H, Moritaka T, Ueda N, Furuya K, Shigematsu S. Bronchial atresia: report of a case and review of the literature. Surg Today 1993; 23:449–454.
4. Murray GF. Congenital lobar emphysema. Surg Gynecol Obstet 1967; 124:611–625.
5. Kennedy CD, Habibi P, Matthew DJ, Gordon I. Lobar emphysema: long-term follow-up. Radiology 1991; 180:189–193.

6. Plit ML, Blott JA, Lakis N, Murray J, Plit M. Clinical, radiographic and lung function features of diffuse congenital cystic adenomatoid malformation of the lung in an adult. Eur Respir J 1997; 10:1680–1682.
7. Zangwill BC, Stocker JT. Congenital cystic adenomatoid malformation within an extralobar pulmonary sequestration. Pediatr Pathol 1993; 13:309–315.
8. Fraggetta F, Cacciaguerra S, Nash R, Davenport M. Intra-abdominal pulmonary sequestration associated with congenital cystic adenomatoid malformation of the lung: just an unusual combination of rare pathologies? Pathol Res Pract 1998; 194: 209–211.
9. Conran RM, Stocker JT. Extralobar sequestration with frequently associated congenital cystic adenomatoid malformation, type 2: report of 50 cases. Pediatr Dev Pathol 1999; 2:454–463.
10. Hellmuth D, Glerant JC, Sevestre H, Remond A, Jounieaus V. Pulmonary adenomatoid malformation presenting as unilobar cysts in an adult. Res Med 1998; 92:1364–1376.
11. Patz EF Jr, Müller NL, Swensen SJ, Dodd LG. Congenital cystic adenomatoid malformation in adults: CT findings. J Comput Assist Tomogr 1995; 19:361–364.
12. Raymond GS, Miller RM, Müller NL, Logan PM. Congenital thoracic lesions that mimic neoplastic disease on chest radiographs of adults. AJR Am J Roentgenol 1997; 168:763–769.
13. Aktogu S, Yuncu G, Halilcolar H, Ermete S, Buduneli T. Bronchogenic cysts: clinicopathological presentation and treatment. Eur Respir J 1996; 9:2017–2021.
14. Patrinou V, Kourea H, Dougenis D. Bronchial carcinoid of an accessory tracheal bronchus. Ann Thorac Surg 2001; 71:1034–1035.
15. McGuinness G, Naidich DP, Garay SM, Davis AL, Boyd AD, Mizrachi HH. Accessory cardiac bronchus: CT features and clinical significance. Radiology 1993; 189:563–566.
16. Ellis K. Developmental abnormalities in the systemic blood supply to the lungs. AJR Am J Roentgenol 1991; 156:669–679.
17. Bouros D, Panagou P, Siafakas N. The varied manifestation of pulmonary artery agenesis in adulthood. Chest 1995; 108:670–676.
18. Gotway MB, Nagai BK, Reddy GP, Patel RA, Higgins CB, Webb RW. Incidentally detected cardiovascular abnormalities on helical CT pulmonary angiography: spectrum of findings. AJR Am J Roentgenol 2001; 176:421–427.
19. Han BK, Dunbar JS, Bove K, Rosenkrantz JG. Pulmonary vascular sling with tracheobronchial stenosis and hypoplasia of the right pulmonary artery. Pediatr Radiol 1980; 9:113–115.
20. Hatten HP Jr, Lorman JG, Rosenbaum HD. Pulmonary sling in the adult. AJR Am J Roentgenol 1977; 128:919–921.
21. Pickhardt PJ. Unilateral lung hypoperfusion with normal ventilation on pulmonary scintigraphy caused by pulmonary artery sling. Clin Nucl Med 1997; 22:484–485.
22. Malmgren N, Laurin S, Lundstrom NR. Pulmonary artery sling: diagnosis by magnetic resonance imaging. Acta Radiol 1988; 29:7–9.
23. Lin JH, Chen SJ, Wu MH, Wang JK, Li YW, Lue HC. Right lung agenesis with left pulmonary artery sling. Pediatr Pulmonol 2000; 29:239–241.
24. Koch A, Hofbeck M, Gerling S, Buheitel G, Singer H. Partial anomalous origin of the left pulmonary artery. Z Kardiol 2000; 89:118–121. [German]
25. Ge S, DeGroff CG, Knudson O, Strain J, Chan KC. Noninvasive assessment of pseudo-pulmonary artery sling by echocardiography and computerized tomography. Circulation 2001; 103: 115–116.
26. Lee JC, Kim GS, Lee SJ, et al. An adult case of pulmonary sling with complete tracheal rings. Korean J Intern Med 1996; 11:175–177.
27. Adler SC, Silverman JF. Anomalous venous drainage of the left upper lobe. Radiology 1973; 108: 563–565.
28. Thorsen MK, Scott JE, Mewissen MW, Youker JE. CT and MR imaging of partial anomalous pulmonary venous return to the azygos vein. J Comput Assist Tomogr 1990; 14:1007–1009.
29. Dillon EH, Camputaro C. Partial anomalous pulmonary venous drainage of the left upper lobe vs. duplication of the superior vena cava: distinction based on CT findings. AJR Am J Roentgenol 1993; 160:375–379.
30. Gilkeson RC, Haaga JR, Ciancibello LM. Anomalous unilateral single pulmonary vein: multidetector CT findings. AJR Am J Roentgenol 2000; 175: 1464–1465.

31. Viamonte M. Intrathoracic extracardiac shunts. Semin Roentgenol 1967; 2:343–367.
32. Swanson KL, Udaya B, Prakash S, Stanson AW. Pulmonary arteriovenous fistulas: Mayo Clinic experience, 1982–1997. Mayo Clin Proc 1999; 74:671–680.
33. Woodring JH, Howard TA, Kanga JF. Congenital pulmonary venolobar syndrome revisited. RadioGraphics 1994; 14:349–369.
34. Ko SF, Ng SH, Lee TY. Anomalous systemic arterialization to normal basal segments of the left lower lobe: helical CT and CTA findings. J Comput Assist Tomogr 2000; 24:971–976.
35. Miller EJ, Singh SP, Cerfolio RJ, Schmidt F, Eltoum IE. Pryce's type I pulmonary intralobar sequestration presenting with massive hemoptysis. Ann Diagn Pathol 2001; 5:91–95.
36. Louie HW, Martin SM, Mulder DG. Pulmonary sequestration: 17-year experience at UCLA. Am Surg 1993; 59:801–805.
37. Stocker JT. Sequestrations of the lung. Semin Diagn Pathol 1986; 3:106–121.
38. Eustace S, Valentine S, Murray J. Acquired intralobar bronchopulmonary sequestration secondary to occluding endobronchial carcinoid tumor. Clin Imaging 1996; 20:178–180.
39. Uppal MS, Kohman LJ, Katzenstein AL. Mycetoma within an intralobar sequestration: evidence supporting acquired origin for this pulmonary anomaly. Chest 1993; 59:801–805.
40. Cerruti MM, Marmolejos F, Cacciarelli T. Bilateral intralobar pulmonary sequestration with horseshoe lung. Ann Thorac Surg 1993; 55:509–510.
41. Hilton TC, Keene WR, Blackshear JL. Intralobar pulmonary sequestration with nutrient systemic arterial flow from multiple coronary arteries. Am Heart J 1995; 129:823–826.
42. Hekelaar N, Van Uffelen R, Van Vliet AC, Varin OC, Westenend PJ. Primary lymphoepithelioma-carcinoma within an intralobar pulmonary sequestration. Eur Respir J 2000; 16:1025–1027.
43. Rappaport DC, Herman S, Weisbrod G. Congenital bronchopulmonary diseases in adults: CT findings. AJR Am J Roentgenol 1994; 162:1295–1299.
44. Au VW, Chan JK, Chan FL. Pulmonary sequestration diagnosed by contrast enhanced three-dimensional MR angiography. Br J Radiol 1999; 72:709–711.
45. Gupta SK, Abraham KA, Ganesh KM. Intralobar sequestration of upper lobe of right lung: case reports. Angiology 1988; 39:1056–1060.
46. Hoeffel JC, Bernard C. Pulmonary sequestration of the upper lobe in children. Radiology 1986; 160:513–514.
47. Ke FJ, Chang SC, Su WJ, Perng RP. Extralobar pulmonary sequestration presenting as an anterior mediastinal tumor in an adult. Chest 1993; 104: 303–304.
48. Samuel M, Burge DM. Extralobar intra-abdominal pulmonary sequestration. Eur J Pediatr Surg 1996; 6:107–109.
49. Baker EL, Gore RM, Moss AA. Retroperitoneal pulmonary sequestration: computed tomographic findings. AJR Am J Roentgenol 1982; 5:956–957.
50. Rosado-de-Christenson ML, Frazier AA, Stocker JT, Templeton PA. Extralobar sequestration: radiologic-pathologic correlation. RadioGraphics 1993; 13:425–441.
51. Kirks DR, Griscom NT. Diagnostic imaging in infancy and childhood. Philadelphia, Pa: Lippincott-Raven, 1998.

This article meets the criteria for 1.0 credit hour in category 1 of the AMA Physician's Recognition Award. To obtain credit, see accompanying test at http://www.rsna.org/education/rg_cme.html.